

Synthesis, crystal structures and magnetic characterization of four β -diketonate-alkoxide iron(III) dimers. Dependence of the magnetic properties on geometrical and electronic parameters

Florence Le Gall ^a, Fabrizia Fabrizi de Biani ^b, Andrea Caneschi ^c, Patrizia Cinelli ^c,
Andrea Cornia ^d, Antonio C. Fabretti ^d, Dante Gatteschi ^{c,*}

^a Department of Chemistry, Université de Rennes, Rennes, France

^b Dipartimento di Chimica, Università degli Studi di Siena, Siena, Italy

^c Dipartimento di Chimica, Università degli Studi di Firenze, Via Maragliano 75, 50144 Florence, Italy

^d Dipartimento di Chimica, Università degli Studi di Modena, Modena, Italy

Received 20 August 1996; revised 5 November 1996; accepted 2 December 1996

Abstract

Synthesis, crystallographic characterization and magnetic properties of the dinuclear iron(III) complexes $[\text{Fe}(\text{OMe})(\text{dbm})_2]_2$ (**1**), $[\text{Fe}(\text{OMe})(\text{dpm})_2]_2$ (**2**), $[\text{Fe}(\text{OEt})(\text{bpm})_2]_2$ (**3**) and $[\text{Fe}(\text{OProp})(\text{npm})_2]_2$ (**4**) are reported. Complexes **1** and **2** have symmetric β -diketonate ligands dbm (dibenzoylmethanate) and dpm (dipivaloylmethanate), respectively, whereas complexes **3** and **4** contain asymmetric β -diketonate ligands bpm (benzoylpivaloylmethanate) and npm (naphthoylpivaloylmethanate), respectively. Complex **1** crystallizes in the triclinic system, space group $P\bar{1}$ (No. 2), $a=9.634(1)$, $b=10.946(2)$, $c=13.079(1)$ Å, $\alpha=79.95(1)$, $\beta=88.01(1)$, $\gamma=82.57(1)^\circ$, $Z=1$. Complex **2** crystallizes in the triclinic system, space group $P\bar{1}$ (No. 2), $a=10.980(2)$, $b=14.255(2)$, $c=17.979(1)$ Å, $\alpha=85.70(1)$, $\beta=89.63(1)$, $\gamma=71.65(1)^\circ$, $Z=2$. Compound **3** crystallizes in the monoclinic system, space group $P2_1/c$ (No. 14), $a=11.546(2)$, $b=18.539(1)$, $c=13.595(2)$ Å, $\beta=113.18(1)^\circ$, $Z=2$. Compound **4** crystallizes in the monoclinic system, $P2_1/c$ (No. 14) space group, $a=13.746(2)$, $b=18.933(2)$, $c=14.158(2)$ Å, $\beta=117.37(1)^\circ$, $Z=2$. Each complex consists of two iron(III) ions that are symmetrically bridged by two alkoxide groups. The antiferromagnetic couplings between the $S=5/2$ iron centers have been fitted by using the Hamiltonian $\mathbf{H}=\mathbf{J}\mathbf{S}_1\cdot\mathbf{S}_2$ to give values of $J=15.4(1)$ cm⁻¹ with $g=1.96(1)$ for **1**, $J=19.0(6)$ cm⁻¹ with $g=1.98(1)$ for **2**, $J=14.8(5)$ cm⁻¹ with $g=1.98(1)$ for **3** and $J=18.0(5)$ with $g=2$ for **4**. The structural and magnetic parameters of **1–4** and other iron(III)-alkoxo clusters synthesized in our laboratory are compared. No simple correlation exists between the isotropic exchange-coupling constant J and the average Fe–O(bridge) bond distance, whereas an approximately linear correlation is found between the J value and the Fe–O–Fe angle. The observed trend and the predictions of Extended Hückel calculations on the model $[\text{Fe}(\text{OH})\text{H}_4]_2^{4-}$ are compared and discussed.

Keywords: Crystal structures; Magnetism; Iron complexes; Alkoxide complexes; Dimeric complexes

1. Introduction

Alkoxide ligands can be successfully used to build up polynuclear metal complexes displaying unusual structures [1,2]. In particular, iron(III)-alkoxo clusters [3–9] are of special interest to material and bioinorganic chemistry [10] because they are naturally related to soluble hydroxo-bridged complexes which act as precursors in the formation of iron oxides [11,12]. Low nuclearity complexes, such as Fe₂ and Fe₃ [4], are likely to represent the ‘molecular bricks’ for the formation of high-nuclearity clusters, and their characteriza-

tion is therefore an essential step for a correct approach to larger systems.

We herein present the synthesis and the structural and magnetic characterization of diiron(III) di(alkoxo)-bridged complexes in which β -diketonates act as ancillary ligands. The reported complexes have been isolated in the course of an extensive investigation of iron(III) solvolytic routes controlled by β -diketonates [3–5] and have general formula $[\text{Fe}(\text{OR})(\text{L})_2]_2$ where R = Me, Et, n-Pr and HL = Hdbm, Hdpm, Hbpm, Hnpm¹. This class of compounds was studied

¹ Abbreviations used in the text: Hdbm = dibenzoylmethane; Hdpm = dipivaloylmethane; Hbpm = benzoylpivaloylmethane; Hnpm = naphthoylpivaloylmethane; H₃salmp = 2-bis(salicylideneamino) methylphenol; Hpm-dbm = 1,3-di(*p*-methoxyphenyl)-1,3-propanedione.

* Corresponding author. Tel.: +39 55-354 841/2/3; fax: +39 55-354 845.

by Gray and co-workers more than twenty years ago, but no X-ray structure determination was performed and only rough estimates of the exchange-coupling constants J were provided [13]. Accurate magnetic measurements down to 3 K have now evidenced a possible correlation between the J values and the Fe–O–Fe angle in the reported dimers and in related Fe₄ and Fe₆ alkoxo-bridged complexes.

2. Experimental

2.1. Synthetic procedures

The starting materials FeCl₃, Hdbm and Hdpm (Aldrich) were used as received. Methanol (Fluka) was dried and distilled over Mg/I₂ under a dinitrogen atmosphere shortly before use. Ethanol and n-propanol (Carlo Erba) were used without further purification. Kopecki's reaction between the appropriate methylester and methylketone in the presence of sodium hydride was used to prepare the ligands Hbpm and Hnmp [14,15]. A two-step procedure was adopted which follows with minor variations that described by Gray and co-workers for the synthesis of [Fe(OMe)(dpm)₂]₂ [13]. Step A is identical for all the reported compounds.

2.1.1. Step A

A 2.37 N solution of MeONa in methanol was prepared by careful addition of metallic Na (2.18 g) to 40 ml of anhydrous methanol. Anhydrous FeCl₃ (0.162 g, 1 mmol) was dissolved in 10 ml of MeOH. The resulting solution was added dropwise to a solution obtained by dissolving HL (1 mmol) in 10 ml of MeOH and 2 ml of the MeONa solution (4.74 mmol MeONa). The yellow-to-red precipitate was isolated by filtration, washed with methanol and dried under vacuum.

2.1.2. Step B for [Fe(OMe)(dbm)₂]₂ (**1**)

The orange–yellow solid obtained in Step A with HL = Hdbm was dissolved in chloroform. Then methanol was carefully layered over the filtered solution and allowed to stand at room temperature, yielding red crystals of **1** in 2–3 days. *Anal.* Calc. for **1**, C₆₂H₅₀O₁₀Fe₂: C, 69.80; H, 4.72; Fe, 10.47. Found: C, 69.42; H, 4.65; Fe, 10.23%.

2.1.3. Step B for [Fe(OMe)(dpm)₂]₂ (**2**)

The bright yellow solid obtained in Step A with HL = Hdpm was dissolved in chloroform. Large orange crystals of **2** were obtained by slow diffusion of methanol vapors. *Anal.* Calc. for **2**, C₄₆H₈₂O₁₀Fe₂: C, 60.94; H, 9.37; Fe, 12.32. Found C, 60.51; H, 9.12; Fe, 12.21%.

2.1.4. Step B for [Fe(OEt)(bpm)₂]₂ (**3**)

The deep-red solid obtained in Step A with HL = Hbpm was dissolved in a 1:1 (vol./vol.) mixture of CHCl₃ and EtOH. Large orange crystals of **3** were obtained either by EtOH vapor diffusion or by slow evaporation. *Anal.* Calc. for

3, C₅₆H₇₀O₁₀Fe₂: C, 66.27; H, 6.95; Fe, 11.01. Found C, 65.89; H, 6.82; Fe, 10.85%.

2.1.5. Step B [Fe(OPr)(npm)₂]₂ (**4**)

The deep-red solid obtained in Step A with HL = Hnmp was dissolved in a 1:1 (vol./vol.) mixture of CHCl₃ and n-PrOH. Orange crystals of **4** were obtained by slow diffusion of n-PrOH vapors. *Anal.* Calc. for **4**, C₇₄H₈₂O₁₀Fe₂: C, 71.5; H, 6.65; Fe, 8.99. Found C, 70.44; H, 6.35; Fe, 8.78%.

2.2. Physical measurements

The magnetic susceptibility of polycrystalline samples was measured by using a Métrologie Ingénierie MSO3 SQUID magnetometer in the temperature range 3–300 K with an applied field of 1 T. Diamagnetic corrections were estimated from Pascal's constants. The magnetic susceptibilities were corrected for the contribution of the sample holder, which was measured separately in the same temperature range and field. An isotropic spin-Hamiltonian defined as $\mathbf{H} = JS_1 \cdot S_2$ ($S_1 = S_2 = 5/2$) was used to fit the experimental data. J and g were treated as adjustable parameters. Corrections for temperature independent paramagnetism were not applied.

2.3. X-ray crystallography

X-ray diffraction studies were performed with an Enraf-Nonius CAD4 diffractometer and graphite monochromatized radiation. The selected crystal of compound **1** was mounted on the top of a glass fiber, whereas a large individual of **2** was sealed in a quartz capillary; both crystals were collected at room temperature; crystals of **3** and **4** were bathed in a stream of cold dinitrogen as soon as they were removed from their mother solution, were mounted on a quartz fiber with silicone grease and collected at 210 and 160 K, respectively. Collected intensities for complexes **1** and **2** were corrected for absorption following the measurements of Ψ scans. Initial heavy atom positions were determined by using the SIR92 program [16] and structures were refined by using the SHELX76 program [17]. Final models were obtained by least-squares refinement in combination with difference Fourier syntheses. Hydrogen atoms were fixed at a C–H distance of 0.95 Å and were assigned isotropic thermal parameters $B = 1.2B_{\text{eq}}(\text{C})$. All non-hydrogen atoms except for the carbon atoms of the alkyl chains in **3** and **4** were refined with anisotropic thermal parameters. The alkyl chains of the bridging propoxide ligands in **4** were subject to major disorder effects and were modeled over two positions: Cx1, Cx2, Cx3, and Cxa, Cxb, Cxc with occupancy factors 0.48 and 0.52, respectively. O–C distances of the propoxide groups were fixed at 1.42 Å. Though a somewhat high thermal parameter resulted for the carbon atom Cx2, the model converged reasonably well. The highest residual peak (0.8 e Å⁻³) was located near Cx2. Crystal data and experimental parameters are reported in Table 1 while atomic coordinates are reported in Tables 2–5.

Table 1

Crystal data and experimental parameters for [Fe(OMe)(dbm)₂]₂ (1), [Fe(OMe)(dpm)₂]₂ (2), [Fe(OEt)(bpm)₂]₂ (3) and [Fe(OPr)(npm)₂]₂ (4)

	1	2	3	4
Formula	Fe ₂ C ₆₂ H ₅₀ O ₁₀	Fe ₂ C ₄₆ H ₈₂ O ₁₀	Fe ₂ C ₅₆ H ₇₀ O ₁₀	Fe ₂ C ₇₄ H ₈₂ O ₁₀
FW (g mol ⁻¹)	1066.77	906.86	1014.86	1243.15
Crystal system	triclinic	triclinic	monoclinic	monoclinic
Space group ^a	<i>P</i> $\bar{1}$ (No. 2)	<i>P</i> $\bar{1}$ (No. 2)	<i>P</i> 2 ₁ / <i>c</i> (No. 14)	<i>P</i> 2 ₁ / <i>c</i> (No. 14)
<i>a</i> (Å)	9.634(1)	10.980(2)	11.546(2)	13.746(2)
<i>b</i> (Å)	10.946(2)	14.255(2)	18.539(1)	18.933(2)
<i>c</i> (Å)	13.079(1)	17.979(1)	13.595(2)	14.158(2)
α (°)	79.95(1)	85.70(1)		
β (°)	88.01(1)	89.63(1)	113.18(1)	117.37(1)
γ (°)	82.57(1)	71.65(1)		
<i>V</i> (Å ³)	1347(3)	2663.2(6)	2675.2(2)	3272.2(2)
<i>Z</i>	1	2	2	2
<i>D</i> _{calc} (g cm ⁻³)	1.315	1.131	1.260	1.262
<i>T</i> (K)	298	298	210	160
λ (Å)	0.71069	1.5418	0.71069	0.71069
Scan type	$\theta-2\theta$	$\theta-2\theta$	$\theta-2\theta$	$\theta-2\theta$
Data collection range (°)	$4 \leq 2\theta \leq 52$	$4 \leq 2\theta \leq 120$	$5 \leq 2\theta \leq 50$	$5 \leq 2\theta \leq 44$
Data limits	$\pm h, \pm k, +l$	$\pm h, \pm k, +l$	$\pm h, +k, +l$	$\pm h, +k, +l$
No. data collected	5509	6193	3949	4369
<i>R</i> _{av}	0.020	0.029	0.066	0.061
No. unique data	4296	4970	2557	3437
No. obs. unique data	2250 with $F_o > 9\sigma(F_o)$	2927 with $F_o > 9\sigma(F_o)$	2143 with $F_o > 16\sigma(F_o)$	2727 with $F_o > 4\sigma(F_o)$
No. parameters	335	454	309	388
Data/parameter ratio	6.7	6.4	6.9	7.0
Absorption coefficient (cm ⁻¹)	5.5	4.7	5.5	4.6
Transmission coefficient, min./max. ^b	0.95/1.00	0.72/1.00		
<i>R</i> ^c	0.048	0.058	0.071	0.096
<i>R</i> _w	0.047	0.063	0.072	0.097
Largest shift/e.s.d., final	0.001	0.001	0.001	0.001
Largest residual peak (e Å ⁻³)	0.29	0.50	0.54	0.61

^a Ref. [44].^b An empirical absorption correction based on ψ scan was applied.^c $R = \sum ||F_o| - |F_c|| / \sum |F_o|$ and $R_w = [\sum w(|F_o| - |F_c|)^2 / \sum w|F_o|^2]^{1/2}$ where $w = 1/\sigma^2(F)$.

Table 2

Final atomic positional parameters^a of [Fe(OMe)(dbm)₂]₂ (1)

Atom	<i>x/a</i>	<i>y/b</i>	<i>z/c</i>
Fe(1)	0.0719(9)	0.3837(7)	0.0718(6)
O(1)	0.1015(4)	0.5570(3)	0.0106(3)
O(2)	-0.0333(4)	0.4256(3)	0.1989(3)
O(3)	0.2417(4)	0.3490(4)	0.1621(3)
O(4)	0.2000(4)	0.3166(3)	-0.0353(3)
O(5)	0.0219(4)	0.2112(3)	0.1119(3)
C(1)	0.2338(6)	0.5965(5)	-0.0138(5)
C(2)	-0.0001(6)	0.3936(5)	0.2937(4)
C(3)	0.1332(6)	0.3358(5)	0.3258(4)
C(4)	0.2477(6)	0.3180(5)	0.2608(4)
C(5)	-0.1107(6)	0.4265(5)	0.3698(4)
C(6)	-0.2243(6)	0.5131(5)	0.3355(5)
C(7)	-0.3259(7)	0.5490(6)	0.4067(5)
C(8)	-0.3158(7)	0.4971(7)	0.5100(5)
C(9)	-0.2058(7)	0.4082(7)	0.5441(5)
C(10)	-0.1028(6)	0.3744(6)	0.4745(5)
C(11)	0.3883(6)	0.2675(5)	0.3038(4)
C(12)	0.4058(7)	0.2077(6)	0.4056(5)

(continued)

Table 2 (continued)

Atom	<i>x/a</i>	<i>y/b</i>	<i>z/c</i>
C(13)	0.5392(8)	0.1626(7)	0.4430(6)
C(14)	0.6537(8)	0.1783(7)	0.3804(6)
C(15)	0.6368(7)	0.2374(7)	0.2796(6)
C(16)	0.5056(7)	0.2797(6)	0.2422(5)
C(17)	0.2556(6)	0.2031(5)	-0.0319(4)
C(18)	0.2131(6)	0.1009(5)	0.0340(4)
C(19)	0.0967(6)	0.1079(5)	0.0995(5)
C(20)	0.3757(6)	0.1876(5)	-0.1061(4)
C(21)	0.4046(7)	0.0799(6)	-0.1501(5)
C(22)	0.5150(8)	0.0700(7)	-0.2203(6)
C(23)	0.5991(8)	0.1607(8)	-0.2451(5)
C(24)	0.5714(7)	0.2666(8)	-0.2025(5)
C(25)	0.4598(7)	0.2806(6)	-0.1323(5)
C(26)	0.0510(6)	-0.0052(5)	0.1631(5)
C(27)	-0.0234(7)	0.0050(6)	0.2545(5)
C(28)	-0.0720(9)	-0.0976(7)	0.3133(7)
C(29)	-0.0499(8)	-0.2124(7)	0.2822(7)
C(30)	0.0211(8)	-0.2239(6)	0.1910(6)
C(31)	0.0728(7)	-0.1227(5)	0.1312(5)

^a Numbers in parentheses are errors in the last significant digit.

Table 3

Final atomic positional parameters ^a for [Fe(OMe)(dpm)₂]₂ (**2**)

Atom	<i>x/a</i>	<i>y/b</i>	<i>z/c</i>
Fe(1)	0.5963(1)	−0.09478(9)	−0.02862(8)
Fe(2)	0.0216(1)	0.09244(9)	0.53101(8)
O(1)	0.5887(5)	0.0286(4)	0.0187(3)
O(2)	0.7878(5)	−0.1501(4)	−0.0197(3)
O(3)	0.5965(5)	−0.1891(4)	0.0603(3)
O(4)	0.5741(6)	−0.2027(4)	−0.0880(3)
O(5)	0.6275(5)	−0.0327(4)	−0.1278(3)
O(6)	0.1116(5)	−0.0294(4)	0.4817(3)
O(7)	−0.0886(6)	0.1982(4)	0.5915(4)
O(8)	0.1005(5)	0.0291(4)	0.6295(3)
O(9)	0.1700(5)	0.1445(4)	0.5220(3)
O(10)	−0.0520(6)	0.1898(4)	0.4422(3)
C(1)	0.6816(8)	0.0781(7)	0.0093(5)
C(2)	0.8575(8)	−0.2328(7)	0.0110(5)
C(3)	0.8104(9)	−0.2953(7)	0.0566(5)
C(4)	0.6822(9)	−0.2713(7)	0.0789(5)
C(5)	0.9985(9)	−0.2567(8)	−0.0076(6)
C(6)	1.014(1)	−0.256(1)	−0.0906(7)
C(7)	1.047(1)	−0.178(1)	0.021(1)
C(8)	1.083(1)	−0.3572(9)	0.0287(8)
C(9)	0.640(1)	−0.3449(7)	0.1324(6)
C(10)	0.718(1)	−0.4509(8)	0.1279(9)
C(11)	0.507(1)	−0.337(1)	0.114(1)
C(12)	0.640(2)	−0.315(1)	0.2076(8)
C(13)	0.6152(9)	−0.2274(7)	−0.1513(6)
C(14)	0.6682(8)	−0.1697(7)	−0.1989(5)
C(15)	0.6707(8)	−0.0759(7)	−0.1871(5)
C(16)	0.609(1)	−0.3282(7)	−0.1715(6)
C(17)	0.704(2)	−0.4058(9)	−0.1268(9)
C(18)	0.618(2)	−0.343(1)	−0.2538(7)
C(19)	0.476(2)	−0.333(1)	−0.1477(9)
C(20)	0.7225(9)	−0.0157(7)	−0.2448(6)
C(21)	0.823(1)	−0.0767(9)	−0.2939(6)
C(22)	0.614(1)	0.0553(9)	−0.2885(7)
C(23)	0.785(1)	0.049(1)	−0.2028(7)
C(24)	0.2455(8)	−0.0796(7)	0.4898(5)
C(25)	−0.0656(9)	0.2245(7)	0.6532(6)
C(26)	0.0356(9)	0.1673(7)	0.7002(6)
C(27)	0.1129(9)	0.0703(7)	0.6867(5)
C(28)	−0.151(1)	0.3249(7)	0.6759(7)
C(29)	−0.286(2)	0.341(1)	0.648(1)
C(30)	−0.162(2)	0.334(1)	0.7561(9)
C(31)	−0.106(2)	0.4003(9)	0.637(1)
C(32)	0.2164(9)	0.0092(7)	0.7443(5)
C(33)	0.158(1)	−0.0574(8)	0.7926(6)
C(34)	0.3277(9)	−0.0562(9)	0.7025(6)
C(35)	0.265(1)	0.0726(8)	0.7934(6)
C(36)	−0.0248(9)	0.2683(7)	0.4214(5)
C(37)	0.0845(9)	0.2871(7)	0.4426(5)
C(38)	0.1789(9)	0.2267(7)	0.4898(5)
C(39)	−0.120(1)	0.3391(7)	0.3657(6)
C(40)	−0.165(2)	0.4415(9)	0.388(1)
C(41)	−0.236(2)	0.311(1)	0.355(2)
C(42)	−0.064(2)	0.353(2)	0.2923(8)
C(43)	0.302(1)	0.2464(7)	0.5058(6)
C(44)	0.317(1)	0.246(1)	0.5897(8)
C(45)	0.311(1)	0.343(1)	0.4722(8)
C(46)	0.411(1)	0.165(1)	0.479(1)

^a Numbers in parentheses are errors in the last significant digit.

Table 4

Final atomic positional parameters ^a for [Fe(OEt)(bpm)₂]₂ (**3**)

Atom	<i>x/a</i>	<i>y/b</i>	<i>z/c</i>
Fe(1)	0.4500(1)	0.0147(8)	0.3796(1)
O(1)	0.5703(5)	0.0533(4)	0.5181(6)
O(2)	0.5939(5)	−0.0302(3)	0.3529(7)
O(3)	0.3393(6)	−0.0383(4)	0.2496(7)
O(4)	0.4694(5)	0.0969(4)	0.2912(6)
O(5)	0.2981(5)	0.0680(4)	0.3775(6)
C(1)	0.5938(9)	−0.0487(5)	0.2618(9)
C(2)	0.4810(8)	−0.0573(5)	0.1700(9)
C(3)	0.3619(1)	−0.0504(6)	0.1677(1)
C(4)	0.4004(1)	0.1511(5)	0.2497(1)
C(5)	0.2891(9)	0.1654(5)	0.2643(1)
C(6)	0.2482(9)	0.1255(6)	0.3314(1)
C(7)	0.7189(8)	−0.0610(5)	0.2599(1)
C(8)	0.8181(9)	−0.0185(6)	0.3187(1)
C(9)	0.9378(1)	−0.0279(8)	0.3160(1)
C(10)	0.9533(1)	−0.0802(8)	0.2521(1)
C(11)	0.8552(1)	−0.1254(7)	0.1920(1)
C(12)	0.7372(1)	−0.1144(6)	0.1922(1)
C(13)	0.1334(1)	0.1485(6)	0.3440(1)
C(14)	0.1282(1)	0.1331(6)	0.4423(1)
C(15)	0.0253(1)	0.1529(7)	0.4677(1)
C(16)	−0.0720(1)	0.1900(8)	0.3930(1)
C(17)	−0.0715(1)	0.2037(7)	0.2931(1)
C(18)	0.0344(1)	0.1843(6)	0.2706(1)
C(19)	0.2469(1)	−0.0614(6)	0.0629(1)
C(20)	0.1724(1)	0.0129(7)	0.0458(1)
C(21)	0.1622(1)	−0.1189(7)	0.0754(1)
C(22)	0.2760(1)	−0.0746(8)	−0.0338(1)
C(23)	0.4410(9)	0.2015(5)	0.1834(1)
C(24)	0.5028(2)	0.1586(8)	0.1225(2)
C(25)	0.3559(1)	0.2537(8)	0.1143(1)
C(26)	0.5535(1)	0.2468(9)	0.2653(1)
C(27)	0.6898(9)	0.0889(6)	0.5303(1)
C(28)	0.6961(1)	0.1613(7)	0.5691(1)

^a Numbers in parentheses are errors in the last significant digit.

2.4. Calculations

Extended Hückel (EH) [18] calculations were performed on the model molecule [Fe(OH)H₄]₂^{4−} in an idealized *D*_{2h} symmetry (see inset in Fig. 8). All the bond distances and angles were fixed to the average of the experimental values apart from the Fe–O–Fe bond angle (θ) which was varied from 115 to 90° along the calculation. The orbital parameters are reported in Table 6. A more complex model like [Fe(OH)(H₂O)₄]₂⁴⁺ was used in trial calculations exploring a few values of θ . The trend in the orbital energies was found consistent with that obtained for [Fe(OH)H₄]₂^{4−}, so justifying the use of the simpler model.

3. Results and discussion

3.1. Synthesis

The reaction of an iron(III) salt with Hdpm and a base in methanol was used many years ago by Gray and co-workers

Table 5
Final atomic positional parameters^a of [Fe(OPr)(npm)₂]₂ (4)

Atom	<i>x/a</i>	<i>y/b</i>	<i>z/c</i>
Fe(1)	0.4575(1)	0.01731(9)	0.3808(1)
O(1)	0.3556(6)	−0.0335(4)	0.2477(6)
O(2)	0.4745(6)	0.0992(4)	0.2979(6)
O(3)	0.3243(6)	0.0693(4)	0.3686(6)
O(4)	0.5802(5)	−0.0262(4)	0.3605(6)
O(5)	0.5574(6)	0.0530(4)	0.5222(5)
C(1)	0.410(1)	0.1452(7)	0.244(1)
C(2)	0.3086(10)	0.1576(6)	0.2416(10)
C(3)	0.2754(9)	0.1205(7)	0.3088(9)
C(6)	0.374(1)	−0.0501(6)	0.169(1)
C(5)	0.4804(10)	−0.0541(6)	0.1790(9)
C(4)	0.5757(10)	−0.0431(6)	0.271(1)
C(7)	0.2676(10)	−0.0627(6)	0.0658(10)
C(15)	0.1705(9)	0.1412(6)	0.3122(10)
C(25)	0.6839(10)	−0.0459(7)	0.271(1)
C(10)	0.294(1)	−0.0730(8)	−0.029(1)
C(22)	0.0200(9)	0.1796(6)	0.3228(10)
C(20)	0.117(1)	0.1958(7)	0.427(1)
C(21)	−0.115(1)	0.1984(6)	0.334(1)
C(18)	0.0714(10)	0.1554(6)	0.513(1)
C(19)	−0.022(1)	0.1743(7)	0.518(1)
C(23)	−0.016(1)	0.1844(6)	0.224(1)
C(24)	0.077(1)	0.1655(7)	0.219(1)
C(31)	0.996(1)	−0.0369(9)	0.279(2)
C(32)	0.883(2)	−0.0436(9)	0.271(1)
C(27)	0.815(1)	−0.0979(9)	0.214(1)
C(17)	0.0742(9)	0.1565(6)	0.4170(10)
C(30)	1.014(2)	−0.086(1)	0.218(2)
C(28)	0.840(2)	−0.1435(8)	0.157(1)
C(29)	0.938(2)	−0.139(1)	0.157(2)
C(33)	0.863(2)	0.0040(8)	0.334(1)
C(34)	0.763(1)	−0.0015(9)	0.332(1)
C(26)	0.704(1)	−0.0973(8)	0.211(1)
C(11)	0.4479(9)	0.1914(6)	0.1771(9)
C(16)	0.1675(9)	0.1342(6)	0.4060(9)
C(9)	0.190(1)	−0.0048(7)	0.046(1)
C(13)	0.554(1)	0.2270(9)	0.253(1)
C(12)	0.460(1)	0.1460(9)	0.097(1)
C(8)	0.2222(10)	−0.1314(6)	0.082(1)
C(14)	0.363(1)	0.2459(8)	0.111(1)
Cx(1)	0.570(3)	0.1272(7)	0.546(3)
Cx(2)	0.680(4)	0.133(3)	0.547(6)
Cx(3)	0.731(3)	0.204(2)	0.591(3)
Cxa	0.664(1)	0.080(1)	0.545(2)
Cxb	0.698(3)	0.151(1)	0.600(2)
Cxc	0.619(3)	0.203(2)	0.524(3)

^a Numbers in parentheses are errors in the last significant digit.

for the synthesis of [Fe(OMe)(dpm)₂]₂ [13]². However, a number of dimer complexes with general formula [Fe(OR)(L)₂]₂ (R = Me, Et, n-Pr; HL = Hdpm, Hbpm, Hnpm) can be easily prepared by similar procedures. When iron(III) chloride is allowed to react with 1 equiv. of

² The same authors described alternative synthetic procedures which involve the reaction of sodium alkoxides with tris(β-diketonate) complexes or oxidation of iron(II) chloride in the appropriate alcohol in the presence of HL. It has recently been demonstrated that under strictly anaerobic conditions the latter reaction leads to the cubane tetrairon(II) clusters [Fe₄(OMe)₄(L)₄(HOMe)₄] (HL = Hdpm, Hdpm) [2a].

β-diketone (HL) and 4–5 equiv. of sodium methoxide in anhydrous methanol, a yellow-to-red precipitate, which analyzes approximately as Fe(OMe)₂(L), is formed. The solid is quite soluble in moderately polar organic solvents such as CHCl₃ and CH₂Cl₂, though insoluble materials are quickly formed when it is exposed to wet air. Slow diffusion of ROH vapors or spontaneous evaporation of a CHCl₃ or CHCl₃/ROH solution lead to dimer complexes **2–4** for R = Me, Et, n-Pr and HL = Hdpm, Hbpm, Hnpm, respectively. It is to be noted that the formation of **3** and **4** involves ligand substitution: methoxide ligands which presumably are present in the starting material are replaced by ethoxide and n-propoxide species, respectively. Complex **1** is formed by liquid diffusion of methanol in a CHCl₃ solution of the appropriate solid obtained in Step A. On the contrary spontaneous evaporation of CHCl₃/MeOH solutions of the same solid leads to the hexairon(III) complex [NaFe₆(OMe)₁₂(dbm)₆]⁺ [3a]. By simply playing with crystallization conditions in Step B we have in fact uncovered a completely new pool of molecular iron(III)–alkoxo clusters [3–5]. Interestingly dbm ligands have allowed the isolation of Fe₂, Fe₃ [4], Fe₄ [19], Fe₆ [3] and Fe₁₀ [5] species from CHCl₃/MeOH mixtures whereas dpm, bpm and npm have so far afforded Fe₂ complexes only. The combined nature of the solvent and of the R' and R'' groups of the β-diketonates (defined as R'–C(O)–CH–C(O)–R'') may therefore play a fundamental role in the aggregation processes.

3.2. Structural studies

Figs. 1–4 display ORTEP [20] views of the four complexes, which have similar structures. The asymmetric unit of **1**, **3** and **4** comprises one half-dimer molecule, whereas the crystal lattice of **2** is generated by two crystallographically independent half-dimers. The two iron(III) ions are related by an inversion center and are symmetrically bridged by two alkoxide groups. The geometry around the metal atoms is roughly octahedral, the six coordination sites being occupied by the oxygen donors of two *cis*-alkoxide groups and two β-diketonate ligands. No evidence was found in either structure for intermolecular contacts between dimer units. The average Fe–O(bridge) bond distances are equal within the experimental errors (see Table 7) and agree well those reported in the literature for similar diiron(III) complexes [21–23]. The Fe–Fe separations vary from 3.049(3) Å for **3** to 3.105 Å for **2**, while the Fe–O–Fe angles range from 101.8(3)° for **3** to 103.7° for **2**. Selected bond distances and angles for compounds **1–4** are reported in Tables 8–11, respectively.

Complexes **1–4** are structurally related to a few iron(III) clusters that contain Fe₂(OR)₂ units, namely [Fe₄(OMe)₆(dpm)₆] (**5**) [19], [NaFe₆(OMe)₁₂(dbm)₆]Cl·CHCl₃·12MeOH (**6**) [3a] and [NaFe₆(OMe)₁₂(pmdbm)₆]ClO₄·*x*CHCl₃·*y*MeOH (**7**) [3b]. Their structures are sketched in Fig. 5. In the tetrairon(III) complex **5** double methoxide bridges connect the central iron(III) ion to the peripheral ones, which are arranged at the vertices of an approximately

Table 6
Valence ionization potential, coefficient and exponents of the atomic Slater functions used in the EH calculations

Atom	Orbital	H_{ii}	c_1	ζ_1	c_2	ζ_2
Fe	4s	-9.17	1.0000	1.900		
	4p	-5.37	1.0000	1.900		
	3d	-12.70	0.5366	5.350	0.6678	1.800
O	2s	-32.30	1.0000	2.275 ^a		
	2p	-14.80	1.0000	2.275		
H	1s	-13.60	1.0000	1.300		

^a The ζ coefficient was altered to 3.050 in the calculation (see text).

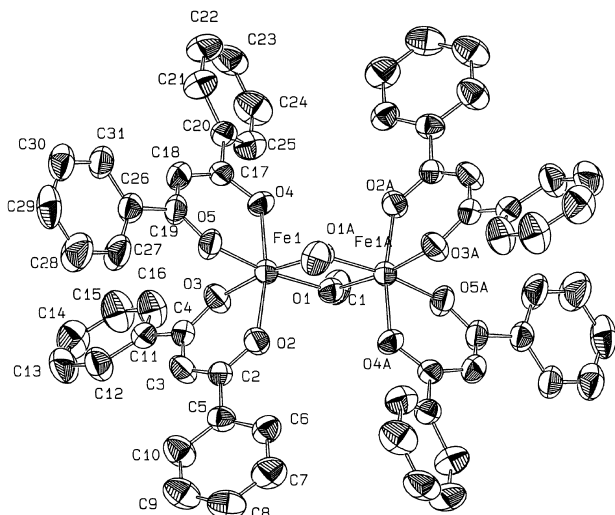


Fig. 1. ORTEP view of the complex $[\text{Fe}(\text{OMe})(\text{dbm})_2]_2$ (1).

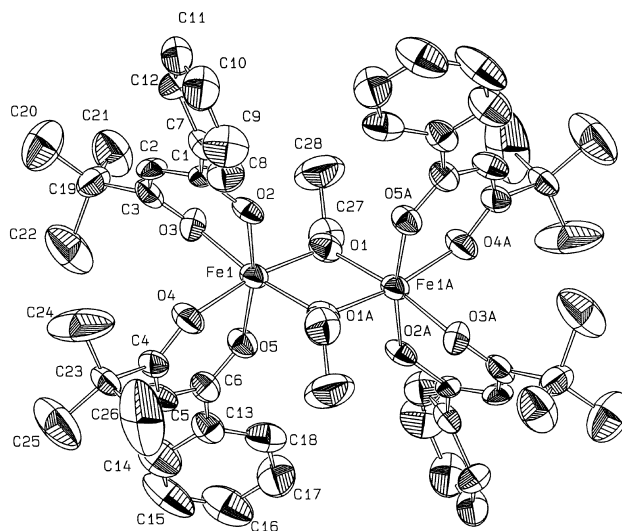


Fig. 3. ORTEP view of the complex $[\text{Fe}(\text{OEt})(\text{bpm})_2]_2$ (3).

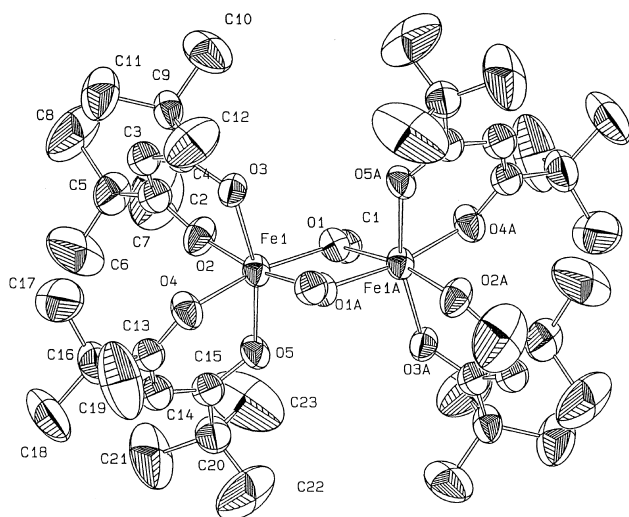


Fig. 2. ORTEP view of the complex $[\text{Fe}(\text{OMe})(\text{dpm})_2]_2$ (2).

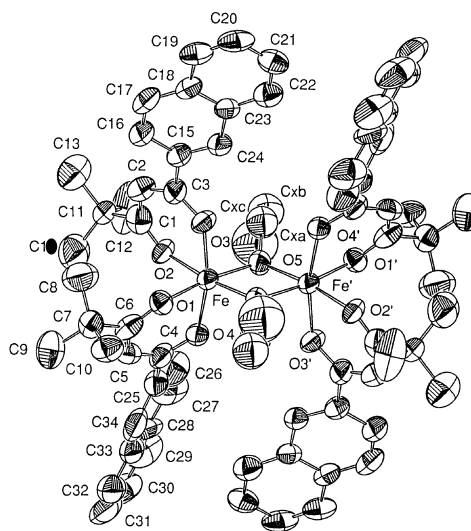


Fig. 4. ORTEP view of the complex $[\text{Fe}(\text{OPr})(\text{npm})_2]_2$ (4).

equilateral triangle and are further coordinated by two β -diketonate ligands (Fig. 5(b)). Hexairon(III) clusters **6** and **7** are isostructural: the metal atoms form a six-membered ring and are connected by double methoxide bridges. In this case only one β -diketonate ligand is found on each metal ion, Fig. 5(c). Interestingly, both clusters encapsulate a sodium ion, which is coordinated by the oxygen atoms of six methoxide ligands.

3.3. Magnetic properties

The temperature dependence of the molar magnetic susceptibility of complexes **1–4** is typical of antiferromagnetically-coupled systems with $S = 0$ in the ground state. Fig. 6 shows the χ versus T plot for compound **3**, but a very similar behavior was observed for compounds **1** and **2**.

Table 7
Structural and magnetic parameters for **1–7**

Compound	Fe–O(bridge) ^c (Å)	Fe···Fe (Å)	Fe–O–Fe (°)	<i>J</i> (cm ⁻¹)	<i>g</i>
[Fe(OMe)(dbm) ₂] ₂ (1)	1.987	3.087(1)	102.0(2)	15.4(1)	1.96(1)
[Fe(OMe)(dpm) ₂] ₂ (2)	1.974	3.105 ^c	103.7 ^c	19.0(6)	1.98(1)
[Fe(OEt)(bpm) ₂] ₂ (3)	1.965	3.049(3)	101.8(3)	14.8(5)	1.98(1)
[Fe(OPr)(npm) ₂] ₂ (4)	1.974	3.093(3)	103.1(5)	18.0(5) ^a	2.00 ^{ab}
[Fe ₄ (OMe) ₆ (dpm) ₆] (5)	1.960	3.133 ^c	105.8 ^c	21.5(3)	1.98(1)
[NaFe ₆ (OMe) ₁₂ (dbm) ₆] ⁺ (6)	2.015	3.195 ^c	104.8 ^c	20.0(3)	2.00 ^b
[NaFe ₆ (OMe) ₁₂ (pmdm) ₆] ⁺ (7)	2.020	3.215(5)	105.6 ^c	19.9(1)	2.00 ^b

^a Values obtained by fitting only the high temperature data.

^b The value was kept fixed.

^c Averaged value.

Table 8
Selected bond lengths (Å) and angles (°) for [Fe(OMe)(dbm)₂]₂ (**1**)^a

O1–Fe1	1.978(3)	O4–Fe1	2.007(3)
O2–Fe1	2.007(4)	O5–Fe1	1.986(4)
O3–Fe1	2.007(4)	O1'–Fe1	1.995(3)
Fe1···Fe1	3.087(1)		
Fe1–O1–Fe1'	102.0(2)	O2–Fe1–O5	87.7(2)
O1–Fe1–O1'	80.0(2)	O2–Fe1–O1'	89.2(1)
O1–Fe1–O2	96.5(1)	O3–Fe1–O4	85.2(2)
O1–Fe1–O3	95.8(2)	O3–Fe1–O5	93.5(2)
O1–Fe1–O4	90.8(1)	O3–Fe1–O1'	171.4(2)
O1–Fe1–O5	170.1(2)	O4–Fe1–O5	86.5(1)
O2–Fe1–O3	85.5(1)	O4–Fe1–O1'	100.8(1)
O2–Fe1–O4	168.7(1)	O5–Fe1–O1'	93.1(1)

^a Numbers in parentheses are errors in the last significant digit.

Table 9
Selected bond lengths (Å) and angles (°) for [Fe(OMe)(dpm)₂]₂ (**2**)^a

O1–Fe1	1.988(5)	O4–Fe1	2.013(6)
O2–Fe1	2.002(6)	O5–Fe1	2.007(5)
O3–Fe1	2.010(5)	O1'–Fe1	1.965(5)
Fe1···Fe1'	3.103(2)		
Fe1–O1–Fe1'	103.7(5)	O2–Fe1–O5	85.3(2)
O1–Fe1–O1	76.6(3)	O1–Fe1–O2	93.8(2)
O1–Fe1–O3	102.2(2)	O3–Fe1–O4	84.6(2)
O2–Fe1–O4	95.7(3)	O3–Fe1–O5	165.0(2)
O1–Fe1–O4	168.8(2)	O1–Fe1–O5	90.0(2)
O2–Fe1–O3	85.1(2)	O4–Fe1–O5	84.9(2)
O1'–Fe1–O2	168.5(3)	O1'–Fe1–O4	94.6(2)
O1'–Fe1–O1	76.6(3)	O1'–Fe1–O3	90.8(2)
O1'–Fe1–O5	100.7(2)		

^a Numbers in parentheses are errors in the last significant digit. The geometrical parameters of the molecule containing Fe2 are equal within the experimental error.

The results of the least-squares fitting of the experimental susceptibility data and selected geometrical parameters of the Fe₂(OR)₂ units are reported in Table 7 for complexes **1–4**. Complex **4** shows a rather unusual χ versus *T* curve for an iron(III) dimer. The susceptibility increases on cooling down from room temperature, seems to approach a broad maximum around 100 K but then increases rather rapidly and passes

Table 10
Selected bond lengths (Å) and angles (°) for [Fe(OEt)(bpm)₂]₂ (**3**)^a

O1–Fe1	1.971(9)	O4–Fe1	2.007(9)
O2–Fe1	2.015(1)	O5–Fe1	2.005(1)
O3–Fe1	1.986(9)	O1'–Fe1	1.959(8)
Fe1···Fe1'	3.049(3)		
Fe1–O1–Fe1'	101.8(3)	O2–Fe1–O5	168.7(5)
O1–Fe1–O1'	78.8(9)	O1–Fe1–O2	90.0(1)
O1–Fe1–O3	171.5(2)	O3–Fe1–O4	91.6(1)
O2–Fe1–O4	84.9(6)	O3–Fe1–O5	88.7(3)
O1–Fe1–O4	95.4(5)	O1–Fe1–O5	96.8(5)
O2–Fe1–O3	85.6(6)	O4–Fe1–O5	85.4(5)

^a Numbers in parentheses are errors in the last significant digit.

Table 11
Selected bond lengths (Å) and angles (°) for [Fe(OPr)(npm)₂]₂ (**4**)^a

Fe1–O1	2.001(1)	Fe1–O4	2.011(1)
Fe1–O2	2.025(1)	Fe1–O5	1.958(1)
Fe1–O3	2.020(1)	Fe1–O5'	1.989(1)
Fe1···Fe1'	3.093(3)		
Fe1–O5–Fe1'	103.1(5)	O2–Fe1–O5	92.4(4)
O1–Fe1–O2	96.6(5)	O3–Fe1–O4	167.3(5)
O1–Fe1–O3	95.7(6)	O3–Fe1–O5	86.7(1)
O1–Fe1–O4	92.9(6)	O2–Fe1–O3	85.4(5)
O1–Fe1–O5	170.8(5)	O4–Fe1–O5	86.2(6)
O2–Fe1–O4	84.3(2)		

^a Numbers in parentheses are errors in the last significant digit.

through a narrow maximum at 30 K. The presence of magnetically dilute ferric impurities was detected at the lowest temperatures. The value $J=18.0(5)$ cm⁻¹ reported in Table 7 was obtained by a fit on the high-temperature data with $g=2.00$. Though we have at present no definitive explanation for the magnetic behavior of **4**, we suggest that a structural phase transition may occur.

Experimental and theoretical work [24–28] on alkoxo- and hydroxo-bridged copper(II) and chromium(III) dimers has demonstrated that the substituents R on the bridging ligands OR have a major influence on magnetic coupling, the greater the electron withdrawing power of R the smaller the value of *J*. However, *J* may be influenced by non-bridging

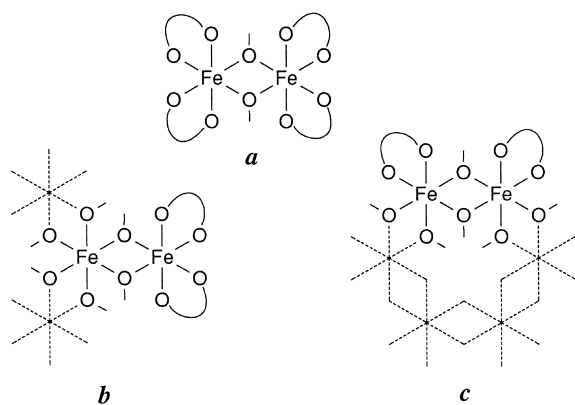


Fig. 5. Sketched structures of dimeric complexes **1–4** (a), and of tetrameric **5** (b) and hexameric **6, 7** (c) clusters. The $\text{Fe}_2(\text{OR})_2$ units are highlighted. Solid arcs represent the β -diketonate ligands.

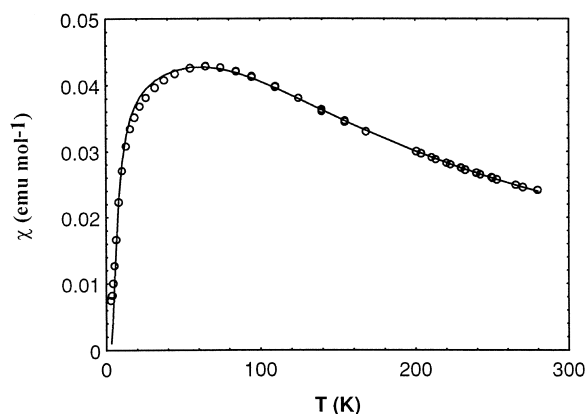


Fig. 6. χ vs. T plot for $[\text{Fe}(\text{OEt})(\text{bpm})_2]_2$ (**3**). The solid line represents the best fit curve.

ligands as well. Inspection of Table 7 shows that the anti-ferromagnetic interactions in complexes **1** ($\text{R} = \text{Me}$; $\text{R}' = \text{R}'' = \text{Ph}$) and **2** ($\text{R} = \text{Me}$; $\text{R}' = \text{R}'' = \text{t-Bu}$) are very similar to each other. Therefore, the influence of R' and R'' on the value of J is probably small. However, J for complex **3** is significantly larger in spite of the fact that $\text{R}' = \text{t-Bu}$ and $\text{R}'' = \text{Ph}$. This is probably due to the different bridging species in **3** ($\text{R} = \text{Et}$) and is in agreement with the stronger electron donating power of Et with respect to Me [24]. A somewhat similar trend is apparent from the rough estimates of J which were reported by Gray and co-workers for related compounds [13].

Complexes **5–7** are structurally similar to **1–4** in that they contain alkoxide and β -diketonate ligands only, and the exchange interactions are invariably mediated by bis(alkoxide) bridges. Inspection of Table 7 shows that they display larger Fe–Fe couplings than **1–4** with J values in the range 19.9–21.5 cm^{-1} (Table 7). In order to rationalize this observation, we tried to correlate the experimental J values with the geometrical parameters of the $\text{Fe}_2(\text{OR})_2$ unit as described in Section 3.4.

3.4. Magneto-structural correlations

Though several attempts to find magneto-structural correlations in iron(III) polynuclear compounds have been made

in the past [29–43], the trend of the J values in weakly coupled systems is still largely unexplained. If one defines the ‘coupling distance’ P as half of the shortest superexchange pathway connecting two metal centers A and B, J_{AB} shows an approximate inverse-exponential dependence upon P [29]. Though it is widely accepted that P has a major influence on the J_{AB} value, plots of J_{AB} against P show a greater scattering of the experimental points when the coupling is small. It has therefore been recognized that when P is large more subtle electronic effects may become important [29]. The classical work on copper(II) and chromium(III) oxo-bridged dimers has inspired a number of investigations on the possible dependence of J_{AB} upon the Fe–O–Fe angle [34,35]. In μ_2 -O bridged non-heme diferric complexes, for which strong couplings are in general observed ($J = 160$ – 240 cm^{-1}), a decrease in the Fe–O–Fe angle leads to a small but significant decrease of J , as pointed out by Kurtz [33]. Some experimental results indicate that the Fe–O–Fe angle may play a role in weakly-coupled systems as well, though a general correlation has not been found. For instance, the ferromagnetic exchange interaction detected in the compound $[\text{Fe}_2(\text{salmp})_2] \cdot 2\text{DMF}$ has been attributed to an unusually acute angle at the bridging OPh ligands ($\approx 97^\circ$) [32]. More recently surprisingly large antiferromagnetic interactions mediated by μ_6 -O bridges have been detected in a few hexairon(III) clusters ($J = 19.0$ – 24.5 cm^{-1} with $P = 2.25(1)$ and Fe–O–Fe = 180°) [7,8].

The stronger couplings found in **5–7** with respect to **1–4** cannot be due to different Fe–O(bridge) distances, since these compounds exhibit larger Fe–O(bridge) separations than **1–4** (see Table 7). Indeed a plot of J versus Fe–O(bridge) distances does not reveal any particular trend. On the contrary a nice linear correlation was found between J and the Fe–O–Fe angle θ (Fig. 7), an increase of the latter leading to a larger J value. The best-fit straight line through the experimental points is

$$J = 1.48\theta - 135$$

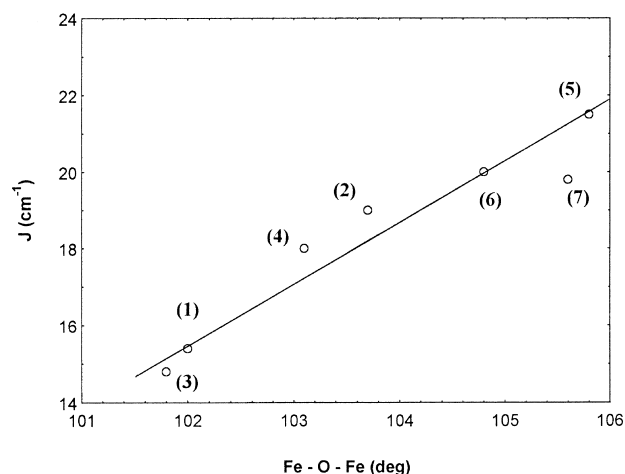


Fig. 7. Plot of the experimental J values vs. the Fe–O–Fe angle θ . The best fit line $J = 1.48\theta - 135$ is also drawn.

According to the above equation, the change of sign of J (i.e. the crossover from antiferro- to ferromagnetic interaction) occurs for $\theta=91^\circ$, in good agreement with the predictions of a simple angular-overlap model.

3.5. Extended Hückel calculations

As shown in Section 3.4, larger Fe–O–Fe angles are associated with stronger antiferromagnetic interactions in our series of compounds. Since for small angles (and short Fe···Fe separations) direct interactions between metal orbitals are expected to enhance antiferromagnetic coupling, the observed trend suggests that indirect interactions predominate. In order to theoretically support these observations we performed EH calculations on the model complex $[\text{Fe}(\text{OH})\text{H}_4]_2^{4-}$ for various values of the Fe–O–Fe angle (θ).

According to the theoretical model developed by Hay et al. [27] the antiferromagnetic contribution J_{AF} to the coupling constant can be studied in terms of pairwise interactions of MOs, holding the relationship $J_{\text{AF}} \propto \sum_i \Delta E_i^2$, where ΔE_i is the energy separation between the symmetric and antisymmetric combinations of couples of magnetic orbitals. Therefore the influence of geometrical distortions on J_{AF} in a series of closely related compounds can be studied by determining the corresponding variation of the quantities ΔE_i . Surprisingly, our calculations predict an increase of $\sum_i \Delta E_i^2$, and hence of J_{AF} , with decreasing Fe–O–Fe angle (Fig. 8(a)). This trend is opposite to the experimental one and suggests prevalent direct interactions. In order to support this conclusion, we performed a calculation on the fragment $[\text{FeH}_4]_2^{2-}$, for which we assumed the same geometry as in the hydroxo-bridged complex. As shown in Fig. 8(c), the quantity $\sum_i \Delta E_i^2$ increases quite rapidly as the two iron atoms approach each other. Hence, at this stage our calculations do

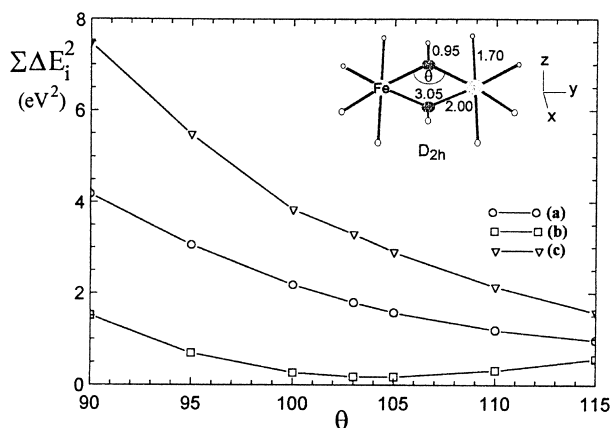


Fig. 8. Plot of $\sum_i \Delta E_i^2$ vs. the Fe–O–Fe angle θ for the $[\text{Fe}(\text{OH})\text{H}_4]_2^{4-}$ model dimer calculated at the EH level by using the orbital parameters reported in Table 6 (a) or with a higher exponent $\zeta=3.05$ for the $2s_{(\text{O})}$ orbital (b). The curve (c) shows the results obtained for the model $[\text{FeH}_4]_2^{2-}$, without the bridging groups. The inset shows a picture of the di(hydroxo)-bridged model with the bond distances (Å) and reference system used in the calculations.

not support the experimental dependence of J upon θ . However, it is well known that the predictions of EH calculations are dramatically influenced by the orbital parameters used. In order to check this point, we repeated the calculation by contracting the $2s_{(\text{O})}$ orbital, so reducing its contribution to the MOs. For this purpose the ζ coefficient of the $2s_{(\text{O})}$ Slater orbital was fixed at 3.05. As previously reported for copper(II) dimers [27], the different angular dependence of the $d_{(\text{Fe})}-s_{(\text{O})}$ and $d_{(\text{Fe})}-p_{(\text{O})}$ overlaps may in fact not have a negligible influence on the trend of J_{AF} . Along with a general lowering of the $\sum_i \Delta E_i^2$ quantity, we found a minimum in the $\sum_i \Delta E_i^2$ versus θ curve at $\theta \approx 104^\circ$ (see Fig. 8(b)). It can therefore be anticipated that by contracting further or even eliminating the $2s_{(\text{O})}$ orbital we can shift the minimum to smaller angles. The model would therefore correctly predict larger J_{AF} values for increasing θ . As already mentioned the same behavior was found in similar Cu(II) dimers [27]; the authors also needed to contract the $2s_{(\text{O})}$ orbital to better reproduce the experimental trend. The origin of such a behavior was explained in terms of the different possibilities of interaction between symmetric and antisymmetric combinations of the metal orbitals and the s and p orbitals of the bridging oxygens, but as a matter of fact no theoretical justification for the necessity to contract the $2s_{(\text{O})}$ orbital was given. It seems that this has to be interpreted as a way to compensate for other weaknesses of the EH approach. It is evident that the results of the EH calculation are strongly influenced by the orbital parameter used; this, together with the presence of ten magnetic orbitals and therefore a large number of magnetic exchange pathways and with a scarceness of homogeneous experimental data, makes any analysis done with such a simple theoretical model difficult.

4. Conclusions

Four diiron(III) complexes **1–4** have been prepared by controlled alcoholysis of iron(III) chloride in the presence of β -diketonates and characterized by single-crystal X-ray diffraction methods. Attention has been focussed on the geometry of the $\text{Fe}_2(\text{OR})_2$ moiety ($\text{R} = \text{Me}, \text{Et}, \text{n-Pr}$) in the solid state and on its influence on the strength of antiferromagnetic coupling. A linear dependence has been found between the J value and the Fe–O–Fe angle in **1–4** and in three other iron(III) polynuclear compounds containing alkoxide and β -diketonate ligands. On the other hand, EH calculations applied to the model developed by Hay et al. [27] do not permit the observed trend to be fully supported. The results of the EH calculation are in fact strongly influenced by the orbital parameters used. This aspect, together with the presence of ten magnetic orbitals and of a large number of magnetic-exchange pathways, makes any analysis done with such a simple theoretical model difficult. Finally, it has to be noted that our EH calculations explored quite a large range of θ values, while the experimental data fall in a small range. The variation in the estimated strength of the

coupling is small as well and could eventually be influenced by other factors. However the homogeneity of the samples, both with respect to the nature of the ligands and to their structural features, supports the thesis of the dependence of the J value on the angle at the bridge in this class of weakly-coupled oxo-bridged polyiron(III) complexes. To our knowledge this represents the first study where such a correlation is well documented by experimental results.

5. Supplementary material

Tables of anisotropic thermal parameters for **1**, **2**, **3**, **4**, SIIa–d (6 pages); coordinates of hydrogen atoms for **1**, **2**, **3**, **4**, SIIIa–d (4 pages); bond distances and angles for **1**, **2**, **3**, **4**, SIIIa–d (8 pages); structure factors for **1**, **2**, **3**, **4**, SIVa–d (28 pages); Fig. SI, plot of χ versus T for compound **4** (1 page) are available from the authors on request.

Acknowledgements

This work was supported by Ministero della Ricerca Scientifica e Tecnologica (MURST), by Consiglio Nazionale delle Ricerche (CNR) and by the Human Capital and Mobility Program through Contract ERBCHRX-CT20080.

References

- [1] (a) M.I. Khan, Q. Chen, H. Höpe, S. Parkin, C.J. O'Connor and J. Zubieta, *Inorg. Chem.*, **32** (1993) 2929; (b) M. Cavaluzzo, Q. Chen and J. Zubieta, *J. Chem. Soc., Chem. Commun.*, (1993) 131.
- [2] (a) K.L. Taft, A. Caneschi, L.E. Pence, C.D. Delfs, G.C. Papaefthymiou and S.J. Lippard, *J. Am. Chem. Soc.*, **115** (1993) 11753; (b) A. Caneschi, A. Cornia, S.J. Lippard, G.C. Papaefthymiou and R. Sessoli, *Inorg. Chim. Acta*, **243** (1996) 295; (c) K.L. Taft, G.C. Papaefthymiou and S.J. Lippard, *Inorg. Chem.*, **33** (1994) 1510.
- [3] (a) A. Caneschi, A. Cornia and S.J. Lippard, *Angew. Chem., Int. Ed. Engl.*, **34** (1995) 467; (b) A. Caneschi, A. Cornia, A.C. Fabretti, S. Foner, D. Gatteschi, R. Grandi and L. Schenetti, *Chem. Eur. J.*, **2** (1996) 1379.
- [4] A. Caneschi, A. Cornia, A.C. Fabretti, D. Gatteschi and W. Malavasi, *Inorg. Chem.*, **34** (1995) 4660.
- [5] A. Caneschi, A. Cornia, A.C. Fabretti and D. Gatteschi, *Angew. Chem., Int. Ed. Engl.*, **34** (1995) 2716.
- [6] V.S. Nair and K.S. Hagen, *Inorg. Chem.*, **31** (1992) 4048.
- [7] (a) K. Hegetschweiler, H.W. Schmalle, H.M. Streit and W. Schneider, *Inorg. Chem.*, **29** (1990) 3625; (b) K. Hegetschweiler, H.W. Schmalle, H.M. Streit, V. Gramlich, H.-U. Hund and I. Erni, *Inorg. Chem.*, **31** (1992) 1299.
- [8] (a) A. Cornia, D. Gatteschi and K. Hegetschweiler, *Inorg. Chem.*, **33** (1994) 1559; (b) A. Cornia, D. Gatteschi, K. Hegetschweiler, L. Hausherr-Primo and V. Gramlich, *Inorg. Chem.*, **35** (1996) 4414.
- [9] K.L. Taft, C.D. Delfs, G.C. Papaefthymiou, S. Foner, D. Gatteschi and S.J. Lippard, *J. Am. Chem. Soc.*, **116** (1994) 821.
- [10] D. Gatteschi, A. Caneschi, R. Sessoli and A. Cornia, *Chem. Soc. Rev.*, (1996) 101.
- [11] W. Schneider, *Chimia*, **42** (1988) 9.
- [12] W. Schneider, *Comments Inorg. Chem.*, **3** (1984) 205.
- [13] C.-H.S. Wu, G.R. Rossman, H.B. Gray, G.S. Hammond and H.J. Schugar, *Inorg. Chem.*, **11** (1972) 990.
- [14] S.N. Poelsma, A.H. Servante, F.P. Fanizzi and P.M. Maitlis, *Liq. Cryst.*, **16** (1994) 675.
- [15] K.R. Kopecki, D. Nonhebel, G. Morris and G.S. Hammond, *J. Org. Chem.*, **27** (1962) 1036.
- [16] A. Altomare, M.C. Burla, G. Camalli, G. Cascarano, C. Giacovazzo, A. Guagliardi and G. Polidori, *J. Appl. Crystallogr.*, **27** (1994) 435.
- [17] G.M. Sheldrick, *SHELX76*, program for crystal structure determination, University of Cambridge, Cambridge, UK, 1976.
- [18] CACAO Package, C. Mealli and D. M Proserpio, *J. Chem. Educ.*, **67** (1990) 399.
- [19] A. Caneschi, A. Cornia, A.C. Fabretti, D. Gatteschi, F. Fabrizi de Biani and R. Sessoli, unpublished results.
- [20] C.K. Johnson, ORTEP, *Rep. ORNL-3794*, Oak Ridge National Laboratory, Oak Ridge, TN, 1965.
- [21] J.A. Bertrand, J.L. Breece and P.G. Eller, *Inorg. Chem.*, **13** (1974) 125.
- [22] J.A. Thich, C. Chih Ou, D. Powers, B. Vasiliou, D. Mastropaolo, J.A. Potenza and H.J. Schugar, *J. Am. Chem. Soc.*, **98** (1976) 1425.
- [23] B. Chiari, O. Piovesana, T. Tarantelli and P.F. Zanazzi, *Inorg. Chem.*, **23** (1984) 3398.
- [24] E. Dixon Estes, R.P. Scaringe, W.E. Hatfield and D.J. Hodgson, *Inorg. Chem.*, **16** (1977) 1179, 1605.
- [25] H.E. LeMay, Jr., D.J. Hodgson, P. Pruettingkura and L.J. Theriot, *J. Chem. Soc., Dalton Trans.*, (1979) 781.
- [26] V.H. Crawford, H.W. Richardson, J.R. Wasson, D.J. Hodgson and W.E. Hatfield, *Inorg. Chem.*, **15** (1976) 2107.
- [27] J.P. Hay, J.C. Thibeault and R. Hoffmann, *J. Am. Chem. Soc.*, **97** (1975) 4884.
- [28] R.D. Willett, in R.D. Willet, D. Gatteschi and O. Kahn (eds.), *Magneto-Structural Correlations in Exchange Coupled Systems*, NATO ASI Series C, Vol. 140, 1985, p. 389.
- [29] S.M. Gorun and S.J. Lippard, *Inorg. Chem.*, **30** (1991) 1625.
- [30] J.R. Hart, A.K. Rappé, S.M. Gorun and T.H. Upton, *Inorg. Chem.*, **31** (1992) 5254.
- [31] R.N. Mukherjee, T.D.P. Stack and R.H. Holm, *J. Am. Chem. Soc.*, **110** (1988) 1850.
- [32] B.S. Snyder, G.S. Patterson, A.J. Abrahamson and R.H. Holm, *J. Am. Chem. Soc.*, **111** (1989) 5214.
- [33] D.M. Kurtz, Jr., *Chem. Rev.*, **90** (1990) 585.
- [34] K. Takahashi, Y. Nishida, Y. Maeda and S. Kida, *J. Chem. Soc., Dalton Trans.*, (1985) 2375.
- [35] C.C. Ou, R.G. Wollmann, D.N. Hendrickson, J.A. Potenza and H.J. Schugar, *J. Am. Chem. Soc.*, **100** (1978) 4717.
- [36] C.C. Ou, R.A. Lalancette, J.A. Potenza and H.J. Schugar, *J. Am. Chem. Soc.*, **100** (1978) 2053.
- [37] J.A. Bertrand, J.L. Breece, A.R. Kalyanaraman, G.J. Longand and W.A. Baker, Jr., *J. Am. Chem. Soc.*, **91** (1970) 5233.
- [38] R.G. Wollmann and D.N. Hendrickson, *Inorg. Chem.*, **17** (1978) 926.
- [39] B. Chiari, O. Piovesana, T. Tarantelli and P.F. Zanazzi, *Inorg. Chem.*, **21** (1982) 1396.
- [40] S. Menage and L. Que, Jr., *Inorg. Chem.*, **29** (1990) 4293.
- [41] S.J. Barclay, P.E. Riley and K.N. Raymond, *Inorg. Chem.*, **23** (1984) 2005.
- [42] B. Chiari, O. Piovesana, T. Tarantelli and P.F. Zanazzi, *Inorg. Chem.*, **21** (1982) 2444.
- [43] G.D. Fallon, A. Markiewicz, K.S. Murray and T. Quach, *J. Chem. Soc., Chem. Commun.*, (1991) 198.
- [44] T. Hahn (ed.), *International Tables for X-ray Crystallography*, Reidel, Dordrecht, Netherlands, 1983.